J|A|C|S COMMUNICATIONS

Published on Web 07/09/2009

Exceptional Stability and High Hydrogen Uptake in Hydrogen-Bonded Metal−Organic Cubes Possessing ACO and AST Zeolite-*like* Topologies

Dorina F. Sava,[†] Victor Ch. Kravtsov,[‡] Juergen Eckert,[§] Jarrod F. Eubank,[†] Farid Nouar,[†] and Mohamed Eddaoudi*[,†]

Department of Chemistry, University of South Florida, 4202 East Fowler Avenue (CHE 205), Tampa, Florida 33620, Materials Research Laboratory, University of California, Santa Barbara, California 93106-5121, and Institute of Applied Physics, Academy of Sciences of Moldova, Academy str. 5, MD2028 Chisinau, Moldova

Received April 23, 2009; E-mail: eddaoudi@cas.usf.edu

Metal−organic frameworks (MOFs) have emerged as a unique class of crystalline solid-state materials because of their potential for structural and functional design[1] along with pertinent applications.[2] Our group, among others, has been developing new strategies for constructing metal−organic materials (MOMs). The single-metal-ion-based molecular building block (MBB) approach[3] in particular has shown potential for targeting zeolite-*like* metal−organic frameworks (ZMOFs), a subset of MOMs whose members exhibit properties and topologies akin to inorganic zeolitic materials. Here we present a new approach for deriving ZMOFs that is based on the assembly of metal−organic cubes (MOCs), which may be regarded as double four-member rings (d4Rs). As these are viewed as composite building units in traditional zeolitic materials,[4] they should also be targeted as suitable MBBs to construct ZMOFs based on d4Rs.

Our group has in fact succeeded in obtaining MOCs by implementing the single-metal-ion-based MBB approach. We previously reported the synthesis of MOC-1,[3a] a robust assembly in which ditopic heterofunctional imidazoledicarboxylate ligands constitute the edges of the cubes, while the MBBs comprising the single metal ions occupy their vertices. The additional peripheral coordination sites in MOCs offer the potential for coordination and/or hydrogen bonding, whereby materials with zeolite-*like* topologies based on d4Rs may be targeted.

ZMOFs are of special interest, as they consist of large and extra-large cavities accompanied by a tunability derived from the intra- and/or extra-framework organic components. While considerable efforts have been directed at these complex materials, the synthesis of ZMOFs has proven to be very challenging. One design strategy that has been successfully implemented involves the construction of ZMOFs based on rigid and directional tetrahedral building units (TBUs), which are utilized in combination with appropriate angular heterofunctional ditopic organic ligands (imidazole- and pyrimidinecarboxylates).[5] Herein we probe an alternative avenue toward intended ZMOFs by means of the introduction of a superior level of built-in information[6] prior to the assembly process.

Accordingly, we report the synthesis of two porous materials, MOC-2 (**1**) and MOC-3 (**2**), with ACO and AST zeolite-*like* topologies, respectively, constructed from vertex-to-vertex hydrogen-bonded MOCs. Reaction of $In(NO_3)_3 \cdot 5H_2O$ with 4,5-dicyanoimidazole (4,5-DCIm) in a *N*,*N*′-dimethylformamide (DMF) solution in the presence of piperazine (Pip) afforded a pale-yellow homogeneous microcrystalline material with a dodecahedron morphology, designated as MOC-2 (**1**).[7] The as-synthesized compound, which is stable in water and most organic solvents, was characterized and formulated by single-crystal X-ray diffraction studies as $[In_8(HImDC)_{12}] \cdot (DMF)_6$.[8]

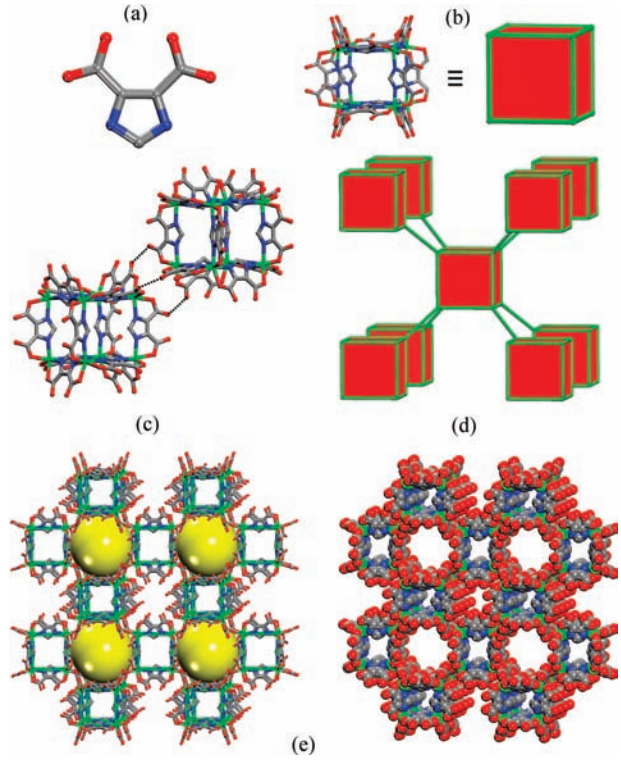

Figure 1. (a) 4,5-Imidazoledicarboxylate (4,5-ImDC) generated in situ from 4.5-DCIm. (b) (left) Ball-and-stick and (right) schematic representations of a MOC. (c) Three O−H···O intermolecular hydrogen bonds linking the vertices of two neighboring cubes. (d) Schematic representation of the ACO topology. (e) Single-crystal X-ray structure of **1** in (left) ball-and-stick and (right) CPK representations. Hydrogen atoms and guest molecules have been omitted for clarity. Color code: In, green; C, gray; N, blue; O, red. Each yellow sphere represents the largest sphere that can be fit inside the cage on the basis of the van der Waals radii.

Each cube consists of 12 doubly deprotonated imidazoledicarboxylate ligands generated in situ[5b,9] that coordinate in a bis(bidentate) fashion to eight In^{3+} metal ions though N-,O- heterocoordination, forming a rigid five-membered chelate ring that locks the metal in its position and reinforces the rigidity and directionality of the assembly. The discrete cubes reside around a special position with $m\bar{3}$ site symmetry, which corresponds to the T_h molecular symmetry of cube. Indium(III) metal ions occupy the vertices of an ideal cube, with In···In distances of 6.675(1) Å and In···In···In angles of 90°.

[†] University of South Florida.
[§] University of California, Santa Barbara.
[‡] Academy of Sciences of Moldova.

10.1021/ja903287v CCC: $40.75

The cubes are connected vertex-to-vertex via intermolecular O−H···O hydrogen bonds (2.786 Å). The three oxygen atoms pointing outward from each vertex of a cube form three intermolecular hydrogen bonds with the corresponding oxygen atoms of the neighboring cube (Figure 1c). That is, each MOC concomitantly connects to eight neighboring ones through 24 hydrogen bonds. It should be noted that all of the carboxylic groups are symmetrically equivalent in the structure, in accordance with the symmetry of the space group, but only one carboxylate can bear the labile proton, so an obvious frustration in the position of the hydrogen atoms involved in the intermolecular hydrogen bonds takes place. One can assume that in each pair of hydrogen-bonded vertices, one vertex donates two protons and accepts one from the neighboring vertex, and vice versa for another vertex of the cube. Moreover, the O···O intramolecular distance of 2.70(1) Å indicates the possibility of intramolecular hydrogen bonds, and thus, the flip-flop model of switching over two possible positions (intermolecular and intramolecular) of the single labile proton on the imidazoledicarboxylate ligand can be addressed.

Consequently, the periodic arrangement of the discrete molecules results in an open framework that resembles the ACO zeolite topology (Figure 1d). The framework exhibits two types of infinite channels and has features and properties similar to those of a compound previously reported by us, with *soc* topology and high hydrogen storage.[10] The first type of channel has small openings with an approximate diameter of 6.373 Å (point-to-point and not including van der Waals radii), while the second type of accessible channel can accommodate a sphere with a maximum diameter of 11.782 Å given the van der Waals radii of the nearest atoms.

The reaction between $In(NO_3)_3 \cdot 5H_2O$ and 4,5-DCIm in EtOH solution yielded colorless polyhedral crystals of a material designated as MOC-3 (**2**),[11] which is insoluble in water and most organic solvents. The as-synthesized compound was characterized and formulated by single-crystal X-ray diffraction studies as $[In_8(HImDC)_{12}][In_8(HImDC)_{11}(ImDC)]^{-}NH_4^{+}$.[12] It is assumed that the proton is transferred from the ImDC carboxylic group to ammonia, thereby implying that every other cube is monoanionic. As in the case of compound **1**, the cubes in the crystal structure of **2** also reside around a special position with $m\bar{3}$ site symmetry, which corresponds to the T_h molecular symmetry of the cube. Additionally, the same ligand coordination to the metal as in **1** is observed. Thus, eight In^{3+} ions occupy the vertices of an ideal cube, with In···In distances of 6.576(2) Å, and are coordinated by 12 exo ligands in a bis(bidentate) fashion. The vertices of four neighboring cubes form a tetrahedral arrangement, generating a cavity in which the ammonium cation resides (Figure S4 in the Supporting Information). The distance from the center of the cavity to each of the 12 surrounding oxygen atoms is 3.207 Å, indicating weak charge-assisted trifurcated N−H···O hydrogen bonding. In this instance, the discrete cubes generate a structure with the AST zeolite topology (Figure 2).

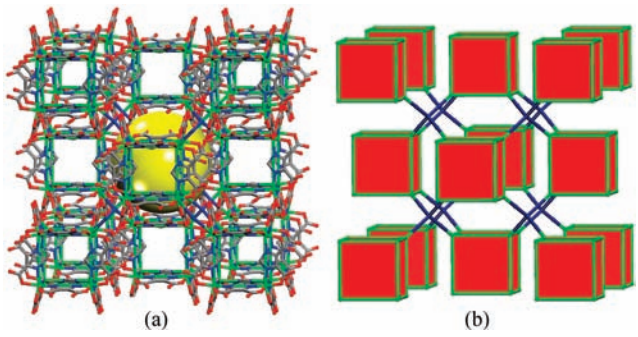

Figure 2. (a) Single-crystal X-ray structure of **2** in the ball-and-stick representation and (b) schematic representation of the AST topology. Hydrogen atoms and guest molecules have been omitted for clarity. Color code: In, green; C, gray; N, blue; O, red. The yellow sphere represents the largest sphere that can be fit inside the cage on the basis of the van der Waals radii.

The total solvent-accessible volumes for **1** and **2** were obtained using the PLATON software by summing voxels that are more than 1.2 Å away from the framework. For **1** this was estimated to be 56.1% of the unit cell volume, while for **2** it represents ∼31%.

Gas-sorption investigations were conducted on the fully evacuated samples after exchange in acetonitrile for 24 h. Nitrogen and argon sorption studies on both **1** (Figure S3a) and **2** (Figure S3b) at 77 and 87 K revealed fully reversible type-I isotherms characteristic of microporous materials. In **1**, the estimated Langmuir surface area was determined to be 1420 $m^2\ g^{-1}$, with a corresponding pore volume of 0.535 $cm^3\ g^{-1}$, as obtained using the Dubinin−Radushkevich (D−R) equation. The estimated Langmuir surface area and pore volume for **2** are 456 $m^2\ g^{-1}$ and 0.1733 $cm^3\ g^{-1}$, respectively, as calculated using the D−R equation.

The porosity of **1** as well as its structural features that resemble the ones observed in *soc*-MOF led us to further evaluate its hydrogen sorption properties. The sample was activated at 135 °C after prior guest exchange in acetonitrile for 24 h. It was evidenced that **1** stores up to 2.17 wt % H_2 at 77 K and atmospheric pressure (Figure 3a). In this context, **1** maintains its integrity upon solvent removal and thermal treatment under vacuum, as evidenced by the sorption isotherms that show no hysteresis upon desorption. This material's exceptional stability and gas-sorption capabilities are remarkable, considering the fact that the framework's skeleton is entirely sustained by hydrogen bonds. The isosteric heat of adsorption was calculated to be 6.5 kJ mol^{-1} and found to be nearly constant at higher loadings, which points to a considerable averaging of the binding sites (Figure S2a).

In order to gain a better understanding of the preferred sorption sites within this material, inelastic neutron scattering (INS) experiments were conducted on **1**. By close inspection of the adsorbed H_2 molecules at different loadings (Figure 3b), many of the spectral features attributable to different binding sites show corresponding increases in intensity with increased loading. The identifiable peaks in the otherwise rather broad INS spectra were assigned (Table S1) on the basis of the same phenomenological model previously used by us.[10] At the lowest loading of 1 H_2/In, the INS spectrum consists of strong peaks at 11 and 14 meV, where the former is accompanied by weaker shoulders at 10 and 11.7 meV. Under the assumption that these transitions are between the two lowest levels of the hindered rotor ("0−1"), we can assign both the 0−2 and 1−2 transitions from the experimental spectrum for four separate binding sites, as listed in Table S1. We also note that there is a very broad "background" underlying the INS spectra, which increases in intensity as a function of hydrogen loading. This part of the spectrum likely arises from random (or nonspecific) site adsorption of H_2 on interior surfaces lined by oxygen atoms, as has been observed in many cases for H_2 in zeolites.[13]

In analogy with our previous work, we attribute the main peak at 11 meV along with the low- and high-energy shoulders to binding sites around the octahedral In metal center. Not all of these faces are in fact accessible to a hydrogen molecule, as is indicated by the fact that the highest total loading in this material at 1 bar (4.6 H_2/In) is far below the value of 8 H_2/In that could in principle be possible. We may assume that the binding energies for the remaining available sites on the octahedron are sufficiently similar

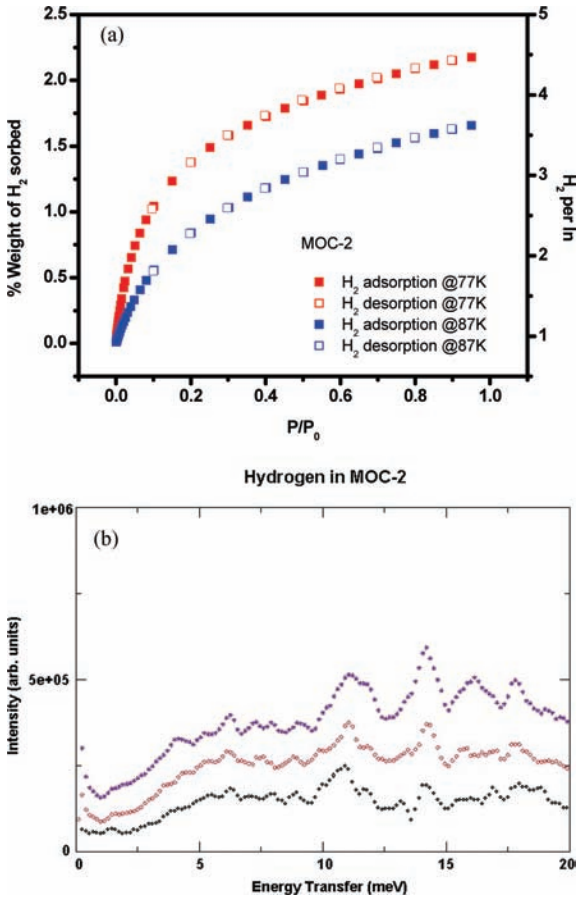

Figure 3. (a) Hydrogen sorption isotherms for **1** at 77 and 87 K and (b) INS spectra of **1** at 15 K for loadings of 1, 2, and 3 H_2/In (the data were obtained on the quasielastic neutron spectrometer at the Intense Pulsed Neutron Source at Argonne National Laboratory).

so that the transitions of hydrogen on all of these can be assigned to this band between 10 and 12 meV.

We note that these sites appear to bind hydrogen slightly more strongly than those around the In carboxylate trimer building block in *soc*-MOF (0−1 transition at 12.8 meV), except for the open binding site on the indium metal ion in the latter material. Peaks associated with hydrogen adsorbed at such a site are indeed absent in MOC-2, as indium is fully coordinated in this case.

The broad band at 14 meV falls into the energy range we have previously assigned to binding sites around organic linking groups. When the hydrogen loading was increased to 2 and 3 H_2 per formula unit, we primarily observed increases in the intensity of existing bands, i.e., changes in the occupancy of the sites described above. This type of behavior is indicative of a small variation in the binding energies of the available sites. It is instructive to refer the loading dependence of the INS spectra to the measured adsorption isotherms and corresponding isosteric heats of adsorption. In the steep portion of the isotherms, more cluster sites are being filled, up to the region between 1 and 2 H_2/In where the slope of the isotherms decreases, at which point more sites on the link are becoming occupied. The result of this is that the average value of the isosteric heat for the system shows a slight decrease.

In summary, here we have reported the synthesis and characterization of two robust porous ZMOFs derived from predetermined MOCs regarded as d4R MBBs, delineating their remarkable stability upon thermal treatment and guest removal in vacuum. Specifically, MOC-2 reveals high hydrogen uptake and qualifies as a suitable platform for studies concerning dihydrogen−framework interactions in the context of a comparative INS study of porous materials possessing similar structural features and properties. INS studies confirmed the overall high capacity of this material originating from the large number of relatively strong binding sites about the metal centers, in combination with small pore sizes, while the ratio of the number of sites around the metal centers to that of the weaker sites around the imidazoles is larger than that in comparable systems.

Further work is being directed toward the construction of ZMOFs derived from a MOC-directed approach, with emphasis on evaluating the effects of pore size and charge density on hydrogen uptake and isosteric heat of adsorption.

Acknowledgment. We gratefully acknowledge the financial support by DOE-BES (DE0FG02-07ER4670) and NSF (DMR 0548117).

Supporting Information Available: IR, XRPD, TGA, INS, and gas-sorption data, structure figures, and X-ray crystallographic data (CIF). This material is available free of charge via the Internet at http://pubs.acs.org.

References

(1) (a) Robson, R. *J. Chem. Soc., Dalton Trans.* **2000**, 3735. (b) Férey, G. *J. Solid State Chem.* **2000**, *152*, 37. (c) Eddaoudi, M.; Moler, D. B.; Li, H.; Chen, B.; Reineke, T. M.; O'Keeffe, M.; Yaghi, O. M. *Acc. Chem. Res.* **2001**, *34*, 319. (d) Moulton, B.; Zaworotko, M. J. *Chem. Rev.* **2001**, *101*, 1629.

(2) (a) Wong-Foy, A. G.; Matzger, A. J.; Yaghi, O. M. *J. Am. Chem. Soc.* **2006**, *128*, 3494. (b) Lee, J.; Farha, O. K.; Roberts, J.; Scheidt, K. A.; Nguyen, S. T.; Hupp, J. T. *Chem. Soc. Rev.* **2009**, *38*, 1450. (c) Alkordi, M. H.; Liu, Y.; Larsen, R. W.; Eubank, J. F.; Eddaoudi, M. *J. Am. Chem. Soc.* **2008**, *130*, 12639. (d) Rieter, W. J.; Pott, K. M.; Taylor, K. M. L.; Lin, W. *J. Am. Chem. Soc.* **2008**, *130*, 11584. (e) Férey, G. *Chem. Soc. Rev.* **2008**, *37*, 191.

(3) (a) Liu, Y.; Kravtsov, V.; Walsh, R. D.; Poddar, P.; Srikanth, H.; Eddaoudi, M. *Chem. Commun.* **2004**, 2806. (b) Liu, Y.; Kravtsov, V. Ch.; Beauchamp, D. A.; Eubank, J. F.; Eddaoudi, M. *J. Am. Chem. Soc.* **2005**, *127*, 7266. (c) Brant, J. A.; Liu, Y.; Sava, D. F.; Beauchamp, D.; Eddaoudi, M. *J. Mol. Struct.* **2006**, *796*, 160.

(4) Baerlocher, C. McCusker, L. B. Database of Zeolite Structures. http://www.iza-structure.org/databases/ (accessed June 18, 2009).

(5) (a) Liu, Y.; Kravtsov, V. Ch.; Larsen, R.; Eddaoudi, M. *Chem. Commun.* **2006**, *14*, 1488. (b) Sava, D. F.; Kravtsov, V. Ch.; Nouar, F.; Wojtas, L.; Eubank, J. F.; Eddaoudi, M. *J. Am. Chem. Soc.* **2008**, *130*, 3768. (c) Eddaoudi, M.; Eubank, J. F.; Liu, Y.; Kravtsov, V. Ch.; Brant, J. A. *Stud. Surf. Sci. Catal.* **2007**, *170*, 2021. (d) Liu, Y.; Kravtsov, V. Ch.; Eddaoudi, M. *Angew. Chem., Int. Ed.* **2008**, *47*, 8446.

(6) (a) Cairns, A. J.; Perman, J. A.; Wojtas, L.; Kravtsov, V. Ch.; Alkordi, M. H.; Eddaoudi, M.; Zaworotko, M. J. *J. Am. Chem. Soc.* **2008**, *130*, 1560. (b) Nouar, F.; Eubank, J. F.; Bousquet, T.; Wojtas, L.; Zaworotko, M. J.; Eddaoudi, M. *J. Am. Chem. Soc.* **2008**, *130*, 1833.

(7) Preparation of **1**: $In(NO_3)_3 \cdot 5H_2O$ (0.087 mmol, 34 mg), 4,5-DCIm (0.1305 mmol, 20.6 mg), DMF (2 mL), Pip (100 μL), and HNO_3/DMF (75 μL) were placed in a 20 mL scintillation vial and heated to 85 °C for 12 h and then 105 °C for 23 h. The pale-yellow, pure, homogeneous microcrystalline material with dodecahedron morphology was collected and air-dried. Yield: 56% based on $In(NO_3)_3 \cdot 5H_2O$.

(8) Crystallographic data for **1**: $C_{65}H_{24}In_8N_{36}O_{50}$; cubic; $Pm\bar{3}n$; $a = 20.195(3)$ Å; $V = 8235.8(18)$ Å^3; $Z = 2$; final R indices [$I > 2\sigma(I)$]: R1 = 0.0442, wR2 = 0.0779.

(9) The in situ hydrolysis of reactants containing cyano groups is known in MOF chemistry. See: Evans, O. R.; Lin, W. *Chem. Mater.* **2001**, *13*, 3009.

(10) Liu, Y.; Eubank, J. F.; Cairns, A. J.; Eckert, J.; Kravtsov, V. Ch.; Luebke, R.; Eddaoudi, M. *Angew. Chem., Int. Ed.* **2007**, *46*, 3278.

(11) Preparation of **2**: $In(NO_3)_3 \cdot 5H_2O$ (0.0435 mmol, 17 mg), 4,5-DCIm (0.1305 mmol, 20.6 mg), EtOH (3 mL), and HNO_3/DMF (200 μL) were placed in a 20 mL scintillation vial and heated to 85 °C for 12 h. Colorless polyhedra were collected and air-dried. Yield: 67% based on $In(NO_3)_3 \cdot 5H_2O$.

(12) Crystallographic data for **2**: $C_{60}H_{50}In_8N_{45}O_{48}$; cubic; $Fm\bar{3}$; $a = 22.418(6)$ Å; $V = 11266(5)$ Å^3; $Z = 4$; final R indices [$I > 2\sigma(I)$]: R1 = 0.0611, wR2 = 0.1503.

(13) Nouar, F.; Eckert, J.; Eubank, J. F.; Forster, P.; Eddaoudi, M. *J. Am. Chem. Soc.* **2009**, *131*, 2864.

JA903287V